

Supplemental Information

**Systemic Virus Infections Differentially Modulate
Cell Cycle State and Functionality of Long-Term
Hematopoietic Stem Cells In Vivo**

Christoph Hirche, Theresa Frenz, Simon F. Haas, Marius Döring, Katharina Borst, Pia-K. Tegtmeyer, Ilija Brizic, Stefan Jordan, Kirsten Keyser, Chintan Chhatbar, Eline Pronk, Shuiping Lin, Martin Messerle, Stipan Jonjic, Christine S. Falk, Andreas Trumpp, Marieke A.G. Essers, and Ulrich Kalinke

Supplementary Figures, Tables & Legends

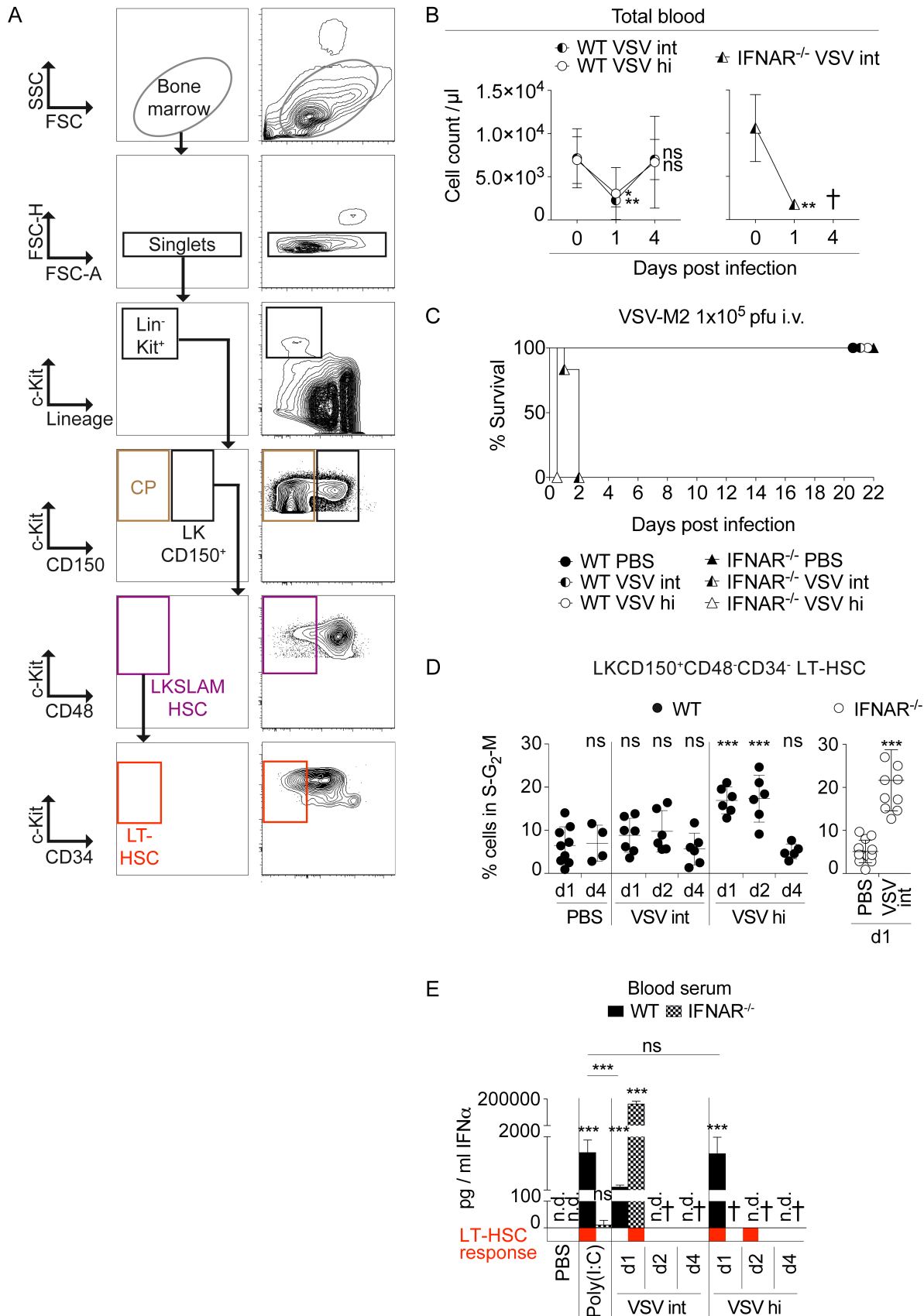


Figure S1 (related to Figure 1):

(A) Flow-cytometry gating strategy for the phenotypic characterization of Lin⁻Kit⁺CD150⁻ committed progenitors (CPs), Lin⁻Kit⁺CD150⁺CD48⁻ hematopoietic stem cells (LKSLAM HSCs) and Lin⁻Kit⁺CD150⁺CD48⁻CD34⁻ long-term hematopoietic stem cells (LT-HSCs) in the murine bone marrow. Stem cell antigen 1 (Sca-1) was excluded from gating to avoid inflammation-induced contamination of investigated bone marrow subsets (see also: Haas et al., 2015). (B) Total blood cell count kinetics of WT and IFNAR^{-/-} mice infected i.v. with either 1x10⁵ PFU VSV (VSV int) or 1x10⁷ PFU VSV (VSV hi) 1 and 4 dpi (n = 5 - 6 ; N = 2). Black cross indicates mice succumbing to infection. (C) Survival kinetics of WT and IFNAR^{-/-} mice infected i.v. with either VSV int or VSV hi (n = 5 - 6 ; N = 2). (D) Kinetics of LT-HSCs in S-G₂-M following i.v. infection of mice with either VSV int (WT and IFNAR^{-/-} mice) or VSV hi (WT mice)(n = 4-9 ; N = 2). (E) IFN-α ELISA of blood sera of mice from (D) (n = 6 ; N = 2). Red boxes below graph indicate coinciding LT-HSC responses (exit from quiescence). Black crosses indicate mice succumbing to infection. Error bars indicate mean±SD, significance determined by two-sided t-test (*, p≤0.05; **, p≤0.0025; ***, p≤0.0001; ns = not significant; n = biological replicates; N = experimental repetitions).

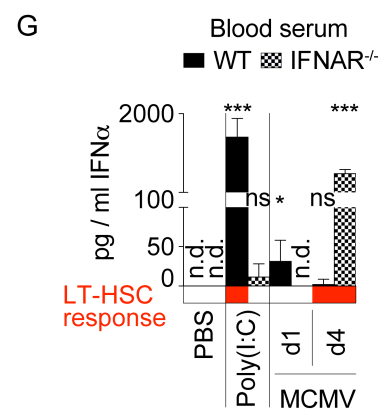
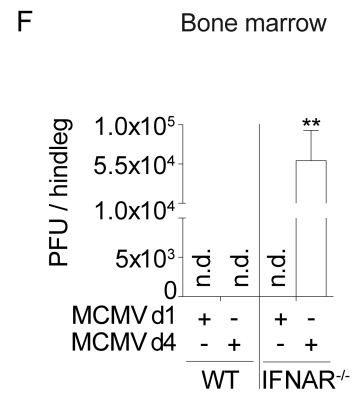
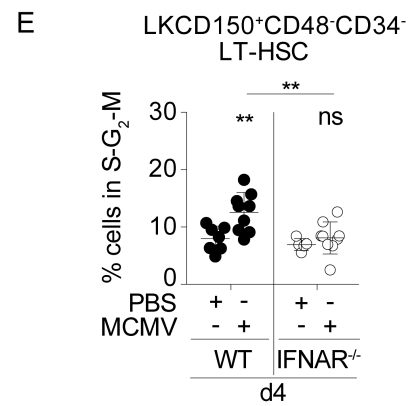
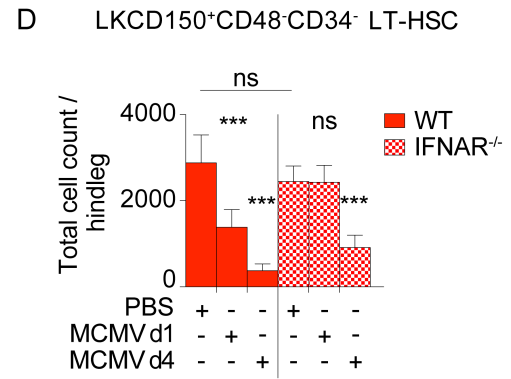
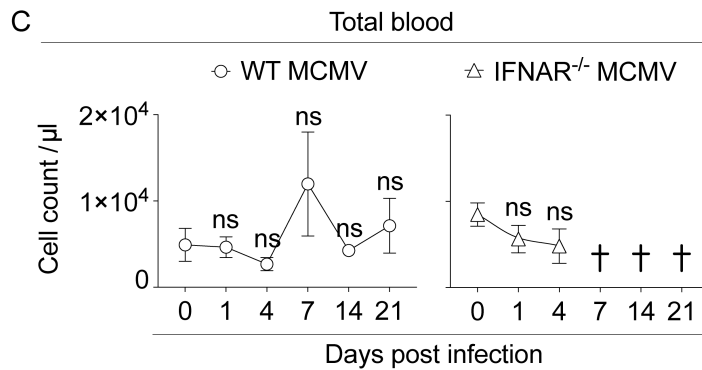
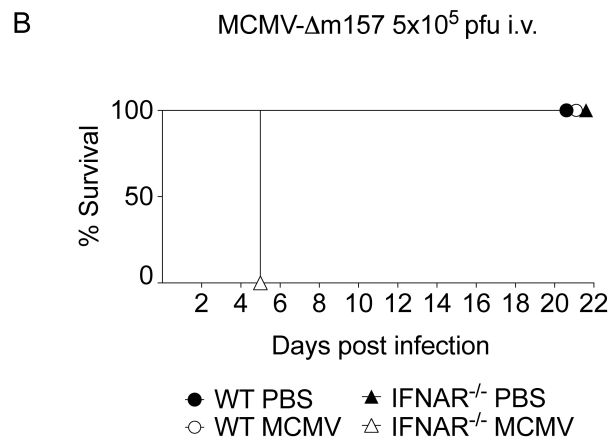
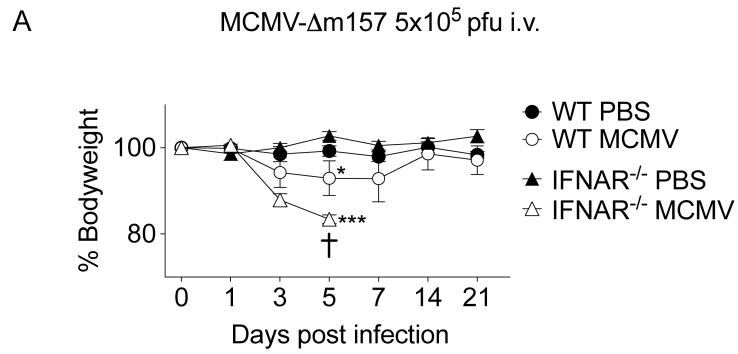


Figure S2 (related to Figure 2):

(A) Weight loss kinetics of WT and IFNAR^{-/-} mice infected i.v. with 5x10⁵ PFU MCMV (n = 3 - 6 ; N = 2). Black cross indicates mice succumbing to infection. **(B)** Survival kinetics of MCMV-infected WT and IFNAR^{-/-} mice (n = 3 - 6 ; N = 2). **(C)** Total blood cell count kinetics of MCMV-infected WT and IFNAR^{-/-} mice (n = 3 - 6 ; N = 2). Black cross indicates mice succumbing to infection. **(D)** Cell count of LT-HSCs of MCMV-infected WT and IFNAR^{-/-} mice 1 and 4 dpi (n = 4-10 ; N = 2). **(E)** Percentages of LT-HSCs in S-G₂-M following MCMV infection of WT and IFNAR^{-/-} mice 4 dpi (n = 5-9 ; N = 2-3). **(F)** Viral titers determined by plaque assay 1 and 4 dpi in bone marrow of MCMV-infected WT and IFNAR^{-/-} mice (n = 6 ; N = 2). **(G)** IFN-α ELISA of blood sera of MCMV-infected WT and IFNAR^{-/-} mice 1 and 4 dpi (n = 6-13 ; N = 2). Red boxes below graph indicate coinciding LT-HSC responses (exit from quiescence). Error bars indicate mean±SD, significance determined by two-sided t-test (*, p≤0.05; **, p≤0.0025; ***, p≤0.0001; ns = not significant; n = biological replicates; N = experimental repetitions).

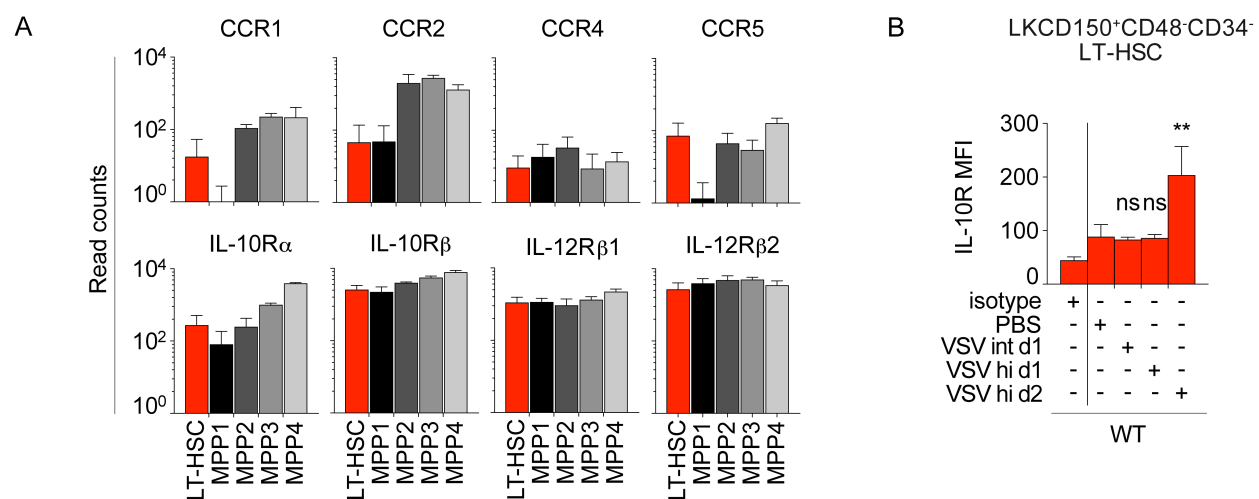


Figure S3 (related to Figure 3):

(A) *In silico* analysis of published transcriptome data of LT-HSCs as well as downstream multipotent progenitor populations (MPP 1-4) (Cabezas-Wallscheid et al., 2014) for the expression of CCL2, CCL3, CCL4 (upper panels) as well as IL-10 and IL-12 (lower panels) cytokine and chemokine receptors. **(B)** IL-10 receptor expression in WT mice following infection with either 1×10^5 PFU VSV (VSV int) or 1×10^7 PFU VSV (VSV hi) at indicated time points ($n = 4-6$; $N = 2$). Error bars indicate mean \pm SD, significance determined by two-sided t-test (*, $p \leq 0.05$; **, $p \leq 0.0025$; ***, $p \leq 0.0001$; ns = not significant; n = biological replicates; N = experimental repetitions).

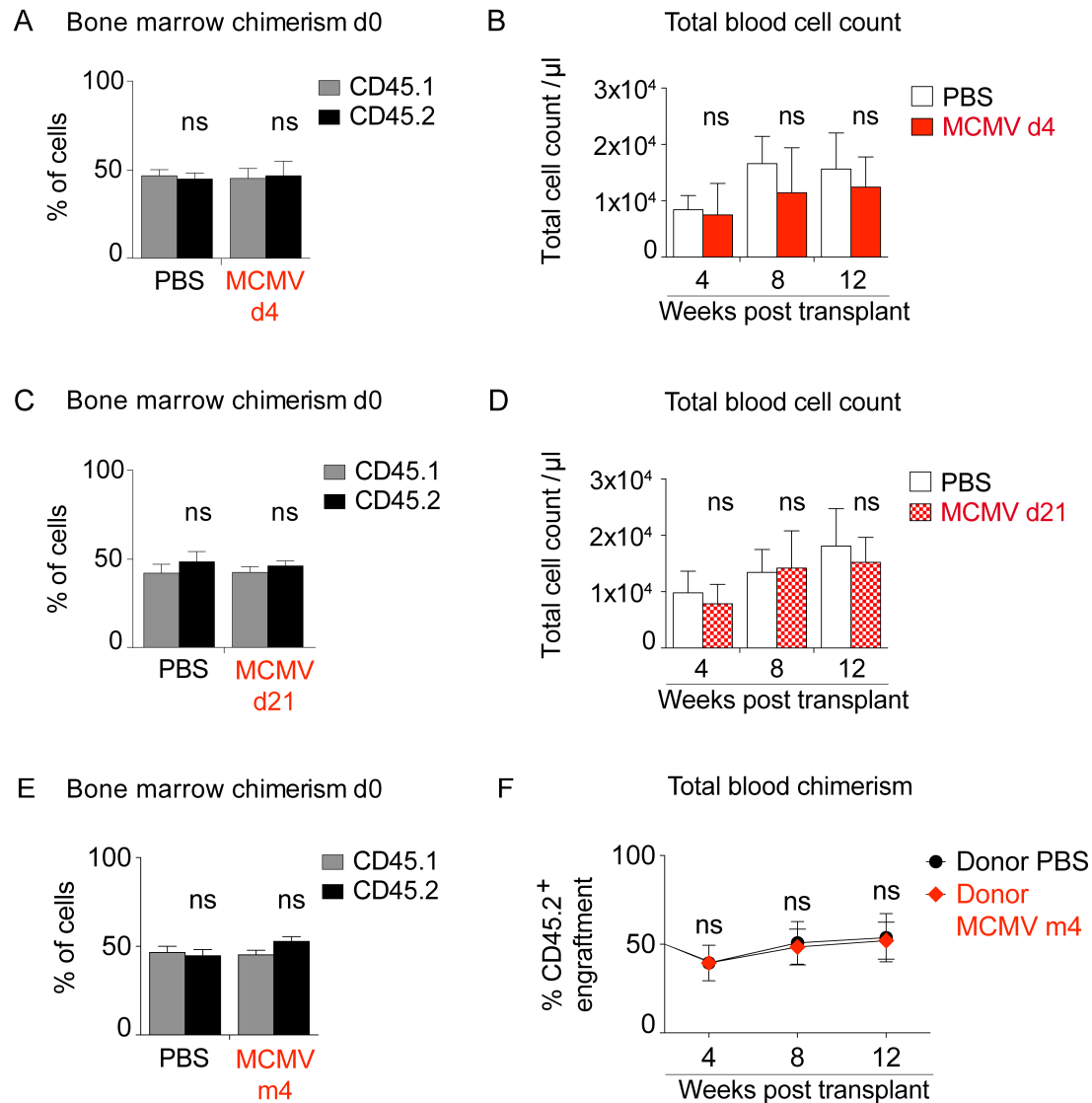


Figure S4 (related to Figure 4):

(A) Chimerism of bone marrow graft mixtures prior to transplantation, set up according to Fig. 6A (5×10^5 PFU MCMV, 4 dpi) ($n = 7-10$; $N = 2$). (B) Total blood cell count post transplantation of (A) ($n = 7-10$; $N = 2$). (C) Chimerism of bone marrow graft mixtures prior to transplantation, set up according to Fig. 6A (5×10^5 PFU MCMV, 21 dpi) ($n = 7-11$; $N = 2$). (D) Total blood cell count post transplantation of (C) ($n = 7-11$; $N = 2$). (E) Chimerism of bone marrow graft mixtures prior to transplantation (left panel), set up according to Fig. 6A from WT mice 4 months post MCMV infection (m4) ($n = 6-7$; $N = 2$). (F) Total blood chimerism post transplantation of (E) ($n = 6-7$; $N = 2$). Error bars indicate mean \pm SD, significance determined by two-sided t-test (*, $p \leq 0.05$; **, $p \leq 0.0025$; ***, $p \leq 0.0001$; ns = not significant; n = biological replicates; N = experimental repetitions).

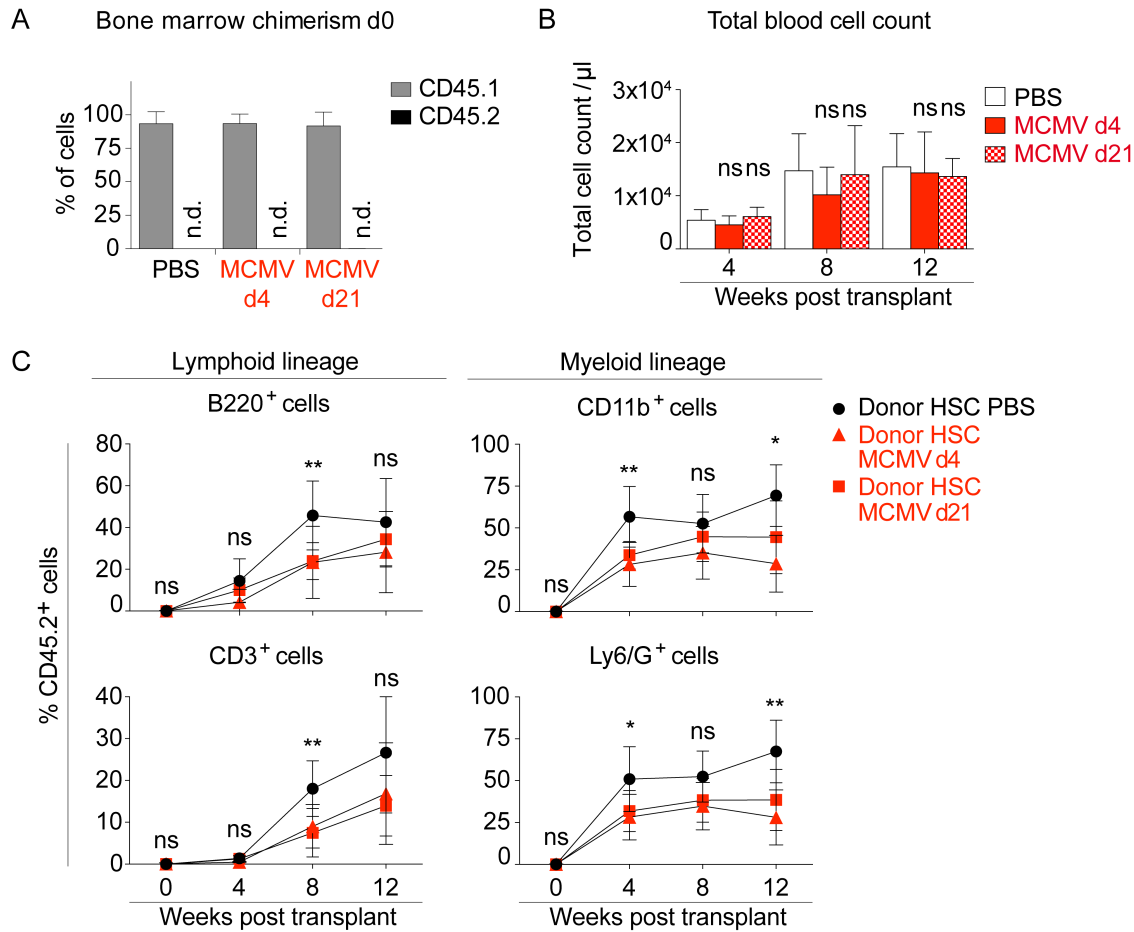


Figure S5 (related to Figure 5):

(A) Chimerism of bone marrow graft mixtures prior to transplantation, set up according to Fig. 6A (5×10^5 PFU MCMV 4 or 21 dpi) ($n = 7-14$; $N = 2$). (B) Total blood cell count post transplantation of (A) ($n = 7-10$; $N = 2$). (C) Contribution of CD45.2⁺ cells to lymphoid (B220⁺, CD3⁺) and myeloid (Ly6/G⁺, CD11b⁺) lineages post transplantation of (A) for mice showing engraftment of more than 5% CD45.2⁺ total blood cells at week 4 ($n = 5-9$; $N = 2$). Error bars indicate mean \pm SD, significance determined by two-sided t-test (*, $p \leq 0.05$; **, $p \leq 0.0025$; ***, $p \leq 0.0001$; ns = not significant; n = biological replicates; N = experimental repetitions).

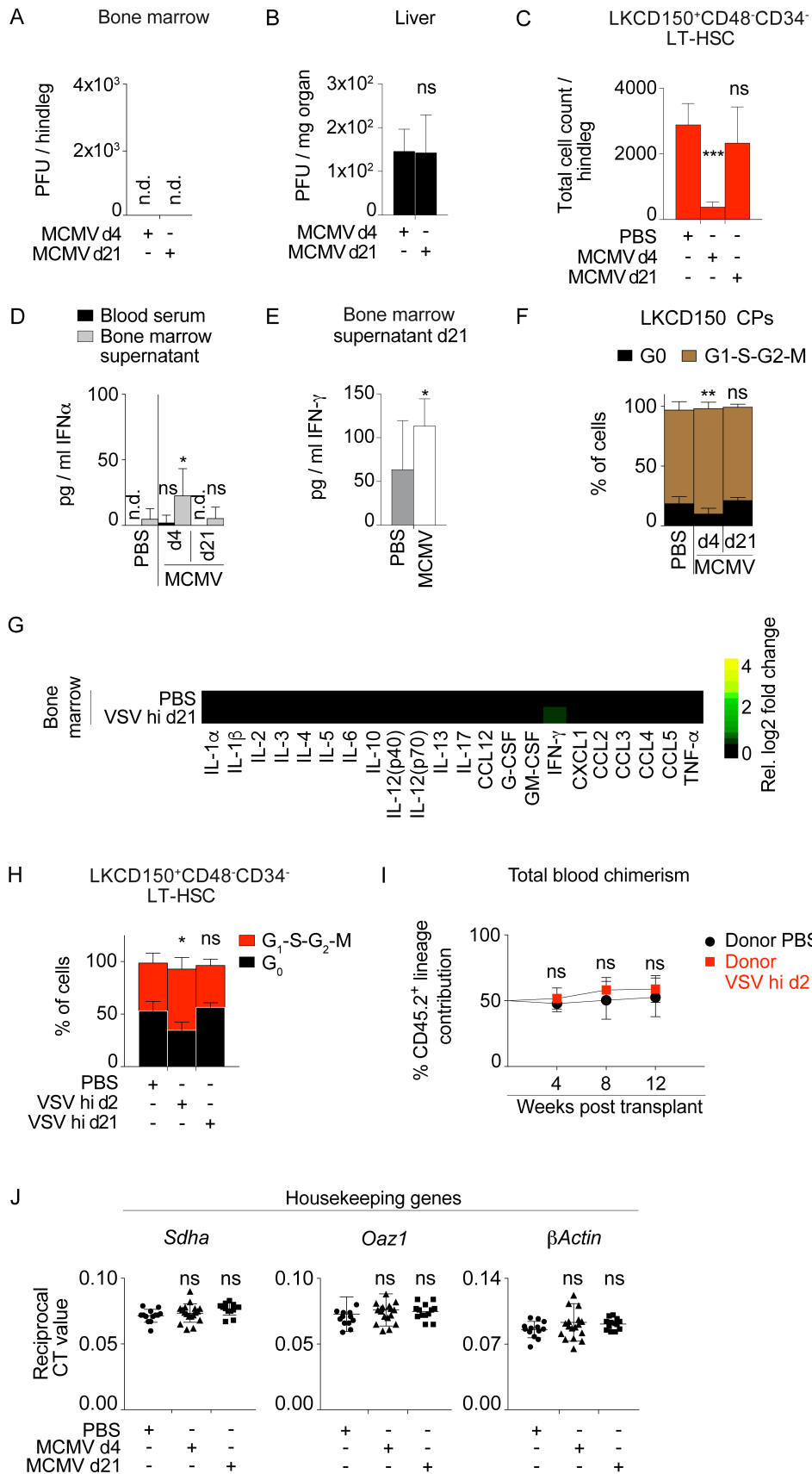


Figure S6 (related to Figure 6):

(A) Viral titers in bone marrow 4 and 21 dpi of WT mice infected i.v. with 5×10^5 PFU MCMV ($n = 6$; $N = 2$). **(B)** Viral titers in livers of MCMV-infected WT mice 4 and 21 dpi ($n = 6$; $N = 2$). **(C)** LT-HSC cell count of MCMV-infected WT mice 4 and 21 dpi ($n = 8-11$; $N = 3$). **(D)** IFN- α ELISA of blood sera and bone marrow supernatants of MCMV-infected WT mice 4 and 21 dpi ($n = 6-13$; $N = 2$). **(E)** IFN- γ ELISA of bone marrow supernatants of MCMV-infected WT mice 4 and 21 dpi ($n = 10$; $N = 2$). **(F)** Intracellular Ki-67/Hoechst staining for quiescent (G_0) and activated (G_1 -S- G_2 -M) committed progenitors (CPs) of MCMV-infected WT mice 4 and 21 dpi ($n = 6-12$; $N = 3$). **(G)** Heat map of multiplex array for 22 cytokines and chemokines in bone marrow supernatants of WT mice 2 and 21 dpi infected i.v. with 1×10^7 PFU VSV-M2 (VSV hi) ($n = 3$; $N = 1$). Data normalized to WT PBS controls. **(H)** Intracellular Ki-67 / Hoechst staining for quiescent (G_0) and activated (G_1 -S- G_2 -M) LT-HSCs of mice from (G) ($n = 6-8$; $N = 2$). **(I)** Total blood chimerism post competitive transplantation of WT total bone marrow 21 dpi VSV hi infection (chimeras set up according to Fig. 4A) ($n = 6-8$; $N = 2$). **(J)** Single-cell RT-qPCR for housekeeping genes to verify gene expression shown in Fig. 6F ($n = 13-18$; $N = 1$). Error bars indicate mean \pm SD, significance determined by two-sided t-test (*, $p \leq 0.05$; **, $p \leq 0.0025$; ***, $p \leq 0.0001$; ns = not significant; n = biological replicates; N = experimental repetitions).

Primer	Sequence
<i>Evi1_fw</i>	AGTTTTCCCGATCTGCAA
<i>Evi1_rev</i>	CCTTGGGACACTGATCACACT
<i>Scl_fw</i>	CAGCCTGATGCTAAGGCAAG
<i>Scl_rev</i>	AGCCAACCTACCATGCACAC
<i>Sca-1_fw</i>	TGGATTCTCAAACAAGGAAAGTAAAGA
<i>Sca-1_rev</i>	ACCCAGGATCTCCATACTTTCAATA
<i>Isg15_fw</i>	TCCTTAATTCCAGGGGACCTA
<i>Isg15_rev</i>	ACCGTCATGGAGTTAGTCACG
<i>Gbp6_fw</i>	CAGGAAGAAGGTTGAACAGGA
<i>Gbp6_rev</i>	GCTCTGAAGGACATGATTTGC
<i>MAT_fw</i>	CCAGCGCGGTTGGAGACGTC
<i>MAT_rev</i>	GACGGGCAGTCGGTCGGATG

Supplemental Table S1: Bulk and single cell qPCR primers (related to Figure 6):

Forward (fw) and reverse (rev) primers utilized in bulk and / or single cell qPCR analyses for respective genes.